Artigo Original

NUMERICAL MODEL OF HEAT TRANSFER IN A REGENERATIVELY COOLED ROCKET ENGINE

Antonio Carlos Foltran[1], Jeremy Paraná Blavier[2]

1. Master in Mechanical Engineering, Federal University of Paraná (UFPR), Curitiba, PR.
2. Mechanical Engineer, Positivo University (UP), Curitiba, PR.

antoniocarlos.foltran@gmail.com, jeremy.blavier91@gmail.com

Keywords
numerical model, rocket engine, regenerative cooling, thermal resistance

Abstract:
In the design phase of rocket engines, the heat transfer problem must be carefully considered in order to prevent chamber wall and coolant temperatures from exceeding its limits. In this paper, the numerical simulation of the steady-state heat transfer in liquid propellant rocket engines by the Centauri program is described. This program uses the quasi-one-dimensional flow theory to calculate the properties of combustion gases and uses a thermal resistances model to calculate the radial heat transfer through the wall into the coolant. The validation of the fluid flow part of the program and the partial validation of the thermal part are also presented.

Paper received in: 22.09.2018
Aproved for publication in: 00.00.2018

INTRODUCTION

In a liquid rocket engine, the burning process occurs inside a combustion chamber, where the propellants are injected, atomized and mixed together. They vaporize and burn and a high pressure is maintained by the expansion of the reacted gases at high temperatures. The combustion products flow from the combustion chamber to a converging-diverging nozzle. In the nozzle region, called throat, the flow reaches the sound speed if sufficient mass flow is provided. Past the throat, the area expansion reduces the pressure and increases flow speed to a supersonic regime. After that, the combustion products are discharged in the atmosphere or vacuum, depending on the medium where the rocket is flying.

The propellant chemical reactions produce gases at high temperatures, in the range of 2500 to 4100 °C (SUTTON; BIBLARZ, 2010). Thus, some cooling mechanism must be provided to prevent the combustion chamber and nozzle walls (which will be henceforth denominated thrust chamber) from overheating. In liquid rocket engines, one of the propellants, normally the fuel, is pressurized to flow inside cooling channels which are machined in the thrust chamber walls. This type of cooling is called regenerative cooling, because the heat is transferred from the combustion gases to the wall and from the wall to the coolant, preventing the wall from overheating. The transferred heat increases the coolant internal energy before its injection in the combustion chamber (SUTTON; BIBLARZ, 2010).

As the flow travels to the thrust chamber exhaust, the combustion products experiment changes in its properties. In addition, the cooling fluid reduces pressure and increases temperature while flowing through the cooling channels. The thermal conductivity of the wall material also presents variation as a function of temperature.

Due to all these phenomena, an analytical solution for the heat transfer problem is impossible to be obtained. That way, a computer program that is able to simulate many cooling channels configurations is desired to produce optimized numerical solutions.

THE NUMERICAL MODEL

Quasi-one-dimensional flow and combustion products properties:

A typical contour of the internal wall of a thrust chamber is shown in FIGURE 1. It can be described as function of longitudinal position measured from the injector plate at the beginning of the combustion chamber, $z = 0$. Referred in this work as a station i, each longitudinal position is associated with its internal radius, wall thickness and cooling channels geometric details. It is easy to see in FIGURE 1 large variations of the internal radius, this promotes large variation in perimeter, so in practical terms the number of cooling channels also varies from combustion chamber to divergent nozzle.

FIGURE 1 – Stations where the radial heat transfer rate and temperatures are calculated.

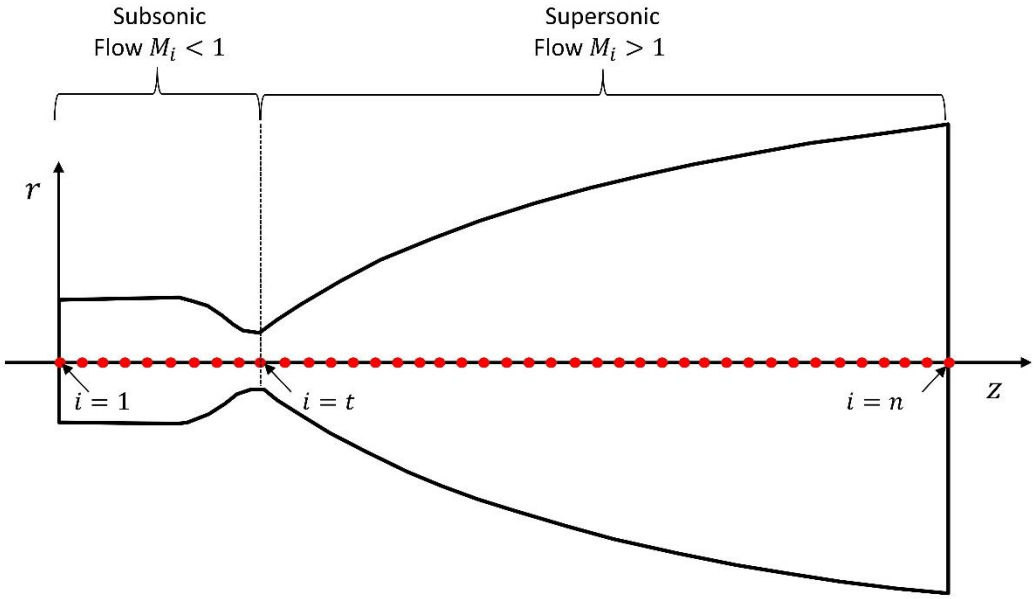

To simulate the combustion gases flow the quasi-one-dimensional flow assumption is made (BORGNAKKE; SONNTAG, 2009). Supposing chocked flow inside the thrust chamber, the Mach number M_i at station i can be found by solving the Eq. (1) with the Bisection Method (CHAPRA; CANALE, 2015)

$$\left[\left(\frac{2}{\gamma_i+1}\right)\left(1+\frac{\gamma_i-1}{2}M_i^2\right)\right]^{(\gamma_i+1)/(\gamma_i-1)}-\left(\frac{A_i}{A^*}M_i\right)^2=0 \quad (1)$$

where A_i is the thrust chamber area normal to the engine axis at station i, A^* is the throat area and γ_i is the ratio of specific heats of the gases mixture at station i.

The throat position is easily found by monitoring the lowest value of the thrust chamber internal radius. Later, the Mach number is found by monitoring the relative position of the station i. If it is before the throat, the Mach number limits used by the Bisection Method are 0 and 1. If the station is after the throat, the limits are 1 and a very large value, for example, 20.

After the calculation of the Mach number, the pressure and temperature of the gases mixture at the corresponding station are calculated by

$$p_i=p_0\left[1+\frac{\gamma_i-1}{2}M_i^2\right]^{-\left(\frac{\gamma_i}{\gamma_i-1}\right)}, \quad (2)$$

$$T_i=T_0\left[1+\frac{\gamma_i-1}{2}M_i^2\right]^{-1}, \quad (3)$$

where p_0 is the stagnation pressure and T_0 is the stagnation temperature.

As the pressure and temperature change while the hot gases flow inside the thrust chamber, its composition and properties varies, including the ratio of specific heats γ. To account for non-constant γ_i, an iterative procedure is conducted. The pressure and temperature in all stations are recalculated successively until a convergence criterion is attained. The user of the code informs the maximum number of iterations and the convergence criterion. A similar procedure was employed in Howell, Strite and Renckel (1965), in terms of modelling the one-dimensional flow that presents large variations in its properties inside a rocket engine.

The gases mixture composition have been found by using the NASA program Chemical Equilibrium with Applications (CEA) (MCBRIDE; GORDON, 1996; GORDON; MCBRIDE, 1994). The version used was the CEARUN available in CEARUN (2016). The simulations use chemical equilibrium in the combustion chamber and "frozen composition" after the throat (variable $nfz=2$). It means the chemical composition does not change downstream the throat.

As the CEA is not coupled to the Centauri program, the results for the interesting thermodynamic and transport properties are given by the CEA output file for relatively few A_i/A^* values selected. Thus, some functions are adjusted to fit these few area ratios and they are directly written in a routine inside the program.

All gases mixture properties were described as functions of temperature in this paper: the ratio of specific heats γ, the thermal conductivity k_g, its dynamic viscosity μ_g, the Prandtl number Pr_g and the specific heat at constant pressure c_p.

The convergence criteria used to stop the iterative process of calculating the combustion gases flow is the L^1 non-dimensional norm of all calculated variables: Mach number, pressure, temperature and ratio of specific heats. When the non-dimensional norms of all properties downs below a tolerance (typically 10^{-10}) the iterative process is considered converged. If the user informs a non-sufficient number of iterations, a warning message appears to the user.

After the convergence of the iterative process, some rocket engine performance parameters can be calculated: gases mixture mass flow $\dot{m}$, characteristic velocity c^*, exhaust velocity V_e, thrust F, specific impulse I_{sp} and thrust coefficient C_F, as defined in Sutton and Biblarz (2010). The sub index n means the exit section of the thrust chamber and $g = 9.80665\ m/s^2$ is the assumed value of the acceleration of gravity at sea level

$$\dot{m} = p_0 A^* \gamma_i \frac{\sqrt{\left[\frac{2}{\gamma_i+1}\right]^{\frac{(\gamma_i+1)}{(\gamma_i-1)}}}}{\sqrt{\gamma_i R T_0}}, \tag{4}$$

$$c^* = \frac{p_0 A^*}{\dot{m}}, \tag{5}$$

$$V_e = M_n \sqrt{\gamma_n R_n T_0}, \tag{6}$$

$$F = \dot{m} V_e + p_n A_n, \tag{7}$$

$$I_{sp} = F/(\dot{m} g), \tag{8}$$

$$C_F = \frac{F}{p_0 A^*}. \tag{9}$$

Once the thermodynamic properties of the combustion gases are calculated, its values hardly change with heat transfer, because the heat losses to the thrust chamber wall is approximately 2% of the chemical energy stored in the propellants (SUTTON; BIBLARZ, 2010). Thus, the combustion gases flow can be assumed as a thermal reservoir.

Thermal resistances model:

A relatively simple, but useful model is employed in this work to describe the heat transfer through the thrust chamber walls. Similar to that described in Naraghi and Foulon (2008), it consists of assuming the heat transfer through the thrust chamber walls as occurring in the radial direction only. It is described as an association of thermal resistances, considering the cooling channels as spaces between a fin set.

The heat transfer in radial direction only can be justified because the wall thickness is much smaller than the thrust chamber wall internal radius. However, some errors are expected at the throat region because the thrust chamber internal radius reaches its minimum and the curvature of the nozzle, combined with large gas properties variations, requires more physical dimensions to describe the heat transfer more precisely.

FIGURE 2 shows a typical cross section of the thrust chamber wall. The cooling channels are machined in the external surface of the internal wall, covered later by the external wall, constituting the thrust chamber. The confined cooling channels conducts the cooling fluid (generally the fuel) in longitudinal direction, following the thrust chamber contour typically from the exhaust to the injection plate. Depending on design, the cooling fluid

can flow through all the thrust chamber length or enters in a manifold generally positioned in some point downstream the throat, making a portion of the divergent nozzle regeneratively cooled and the other part not.

The internal wall material between the channels can be modelled as a fin set. This approach is acceptable because it is made from alloys with good thermal conductivity (e.g. cooper alloys) and the high aspect ratio of the fins produce temperature variations mainly in the radial direction.

In addition, the external wall that covers the channels is less thermal conductive and more robust to withstand the stresses during operation. Generally, it presents a small heat exchange with atmosphere or vacuum, so the fin tip can be modelled as adiabatic. In real rocket engines, this assumption no holds, but it is accepted in this work because the adiabatic fin end calculations are simple.

The convective heat-transfer coefficient must be known when calculating the heat removal by convection. As the cooling fluid flows confined in channels, the relations of internal flow in ducts can be used to estimate the convective heat-transfer coefficient.

As all heat transfer phenomena are considering as occurring in radial direction, the thermal resistance of all heat transfer mechanisms is summed to account for the total thermal resistance (BERGMAN et al., 2011). The first thermal resistance is due to convection in the combustion gases mixture $R_{g,i}$ at station i and given by

$$R_{g,i} = \frac{1}{2\pi r_{1,i} L_i h_{g,i}}, \tag{10}$$

where $r_{1,i}$ is the thrust chamber internal radius as shown in FIGURE 2, L_i is the station i length (calculated as the distances in z and r directions) an $h_{g,i}$ is the gases mixture convective heat-transfer coefficient.

FIGURE 2 – Transversal section of a station showing the thermal resistances model.

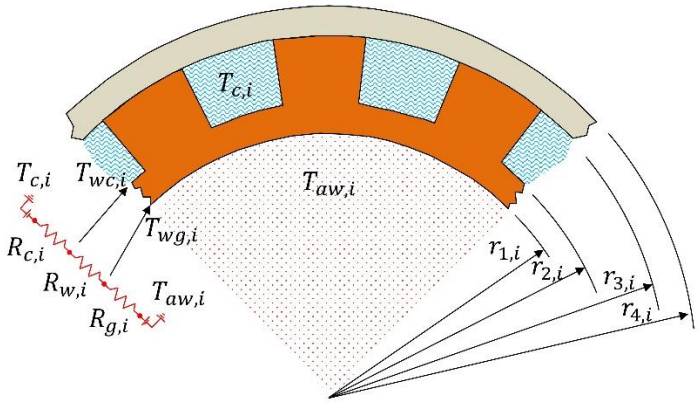

The thermal resistance due to conduction inside the wall material is given by

$$R_{w,i} = \frac{\ln\left(\frac{r_{2,i}}{r_{1,i}}\right)}{2\pi L_i k_{w,i}}, \tag{11}$$

where $r_{2,i}$ is the fin base radius, and $k_{w,i}$ is the wall material termal conductivity (considered as a constant value in this work).

The thermal circuit ends with the coolant fluid convection over the channels exposed surfaces, so the coolant convective heat-transfer coefficient $R_{c,i}$ is

$$R_{c,i} = \frac{1}{\eta_{0,i} A_{t,i} h_{c,i}}, \tag{12}$$

where $h_{c,i}$ is the coolant convective heat-transfer coefficient and $\eta_{0,i}$ is the efficiency of the fin set, given by

$$\eta_{0,i} = 1 - \frac{N_i A_{f,i}}{A_{t,i}}\left(1 - \eta_{f,i}\right), \tag{13}$$

where N_i is the number of fins at the station considered (the program comports variable number of fins at each station) and $A_{f,i}$ is the area of an individual fin.

$A_{t,i}$ is the total area exposed to the coolant at the station i and is given by the sum of the finned area and the fin base exposed area

$$A_{t,i} = N_i A_{f,i} + L_i\left(2\pi r_{2,i} - N_i t_i\right), \tag{14}$$

where t_i is the fin thickness. Assuming that all heat is absorbed by the coolant, the fin efficiency can be calculated by the formula for adiabatic tip condition

$$\eta_{f,i} = \frac{\tanh\left(m_i L_{c,i}\right)}{\left(m_i L_{c,i}\right)}. \tag{15}$$

In Eq. (15) $L_{c,i}$ is the characteristic length of the fin (as the fin tip are in contact with the external wall and not with the coolant, $L_{c,i}$ is the fin length or channel depth). The parameter $m_i = \sqrt{2h_{c,i}/k_f t_i}$ is a fin parameter and k_f is the fin material thermal conductivity, thus the same value used to wall thermal conductivity.

The heat transfer rate q at station i is given by the ratio of fluids temperature difference and the total thermal resistance

$$q_i = \frac{\left(T_{aw,i} - T_{c,i}\right)}{\left(R_{g,i} + R_{w,i} + R_{c,i}\right)}. \tag{16}$$

If the combustion gases are at slow speed, the correct temperature difference to take is $T_i - T_{c,i}$t, but as the combustion gases flows in most stations at supersonic speeds, the reduction of kinetic energy in the boundary layer promotes increase in enthalpy and, consequently, the temperature. This is why the adiabatic wall temperature is used instead of the static value T_i.

The effect is more pronounced in the divergent section, as the flow accelerates considerably while the thrust chamber walls are in rest. The no slip condition at internal wall promotes the deceleration of the flow forming a narrow boundary layer that partially remains at higher temperature than the core flow.

To account to this phenomenon an adiabatic wall temperature $T_{aw,i}$ is calculated

$$T_{aw,i} = T_0 \left[\frac{1+Pr_0^{1/3}\frac{(\gamma_i-1)}{2}M_i^2}{1+\frac{(\gamma_i-1)}{2}M_i^2} \right], \tag{17}$$

where Pr_0 is the Prandtl number at stagnation state (normally taken the value in the beginning of the combustion chamber, where flow speed is small).

The thermal convective heat-transfer coefficient $h_{g,i}$ at station i is given by Bartz (1957) as

$$h_{g,i} = 0.026 \left(\frac{\mu_0}{D^*}\right)^{0.2} \frac{c_{p0}}{Pr_0^{0.6}} \left(\frac{p_0}{c^*}\right)^{0.8} \left(\frac{A^*}{A_i}\right)^{0.9} \sigma_i, \tag{18}$$

where the subindex i differentiates between stations values and the throat value. $D^*$and A^* represent the throat diameter and throat area, respectively. In the Eq. (18) μ_0 is the dynamic viscosity of the gases mixture at the stagnation state and c_{p0} is the constant pressure specific heat, also at stagnation state.

It is important to note that when using Eq. (18) with imperial units, the standard acceleration of gravity appears multiplying p_0 as shown in Bartz 1957. As this work considers the international system units, it does not appear.

The parameter σ_i is given in Bartz (1957) as

$$\sigma_i = \left[\frac{T_{wg,i}}{2T_0}\left(1+\frac{(\gamma_i-1)}{2}M_i^2\right)+\frac{1}{2}\right]^{-0.68} \left[1+\frac{(\gamma_i-1)}{2}M_i^2\right]^{-0.12}, \tag{19}$$

where $T_{wg,i}$ is the internal wall temperature at station i, a value not known *a priori*.

The last variable to be calculated is the convective heat-transfer coefficient of the cooling propellant $h_{c,i}$. It can be modelled by the Sieder and Tate equation (BERGMAN et al., 2011)

$$h_{c,i} = \frac{k_{c,i}}{D_{h,i}} 0.027 Re_{c,i}^{0.8} Pr_{c,i}^{1/3} \left[\frac{\mu_{c,i}}{\mu_{s,i}}\right]^{-0.14}, \tag{20}$$

where $k_{c,i}$, $\mu_{c,i}$ and $Pr_{c,i}$ are the coolant thermal conductivity, kinematic viscosity and Prandtl number, respectively. The variable $\mu_{s,i}$ is the kinematic viscosity of the coolant at cooling channel surfaces temperature (temperature at $r_{2,i}$ as shown in FIGURE 2).

As the surfaces of the cooling channels are not circular, is necessary to specify the hydraulic diameter $D_{h,i}$ before calculating the Reynolds number. Considering fins with constant thickness, the hydraulic diameter is given by

$$D_{h,i} = \frac{4A_{c,i}}{P_i} \approx \frac{4\left[\frac{\pi}{N_i}\left(r_{3,i}^2 - r_{2,i}^2\right) - t_i CCH_i\right]}{2\left[CCH_i + \frac{\pi}{N_i}\left(r_{3,i} - r_{2,i}\right) - t_i\right]}. \tag{21}$$

In Eq. (21), $A_{c,i}$ is the cross section area of one cooling channel at station i, P_i is the wet perimeter and CCH_i is the cooling channel height. Depending on the manufacturing process, the fin thickness is constant or the cooling channel width CCW_i is constant. One can note that constant cooling channel width is more practical to be machined, but Eq. (12) to Eq. (15) were developed considering constant cross section fins. Thus, in this work the fin thickness is chosen to be constant, as exaggeratedly shown in FIGURE 3 and written in mathematical form in the last term in Eq. (21).

FIGURE 3 – If the fin thickness is constant, the cooling channel does not have a rectangular cross section.

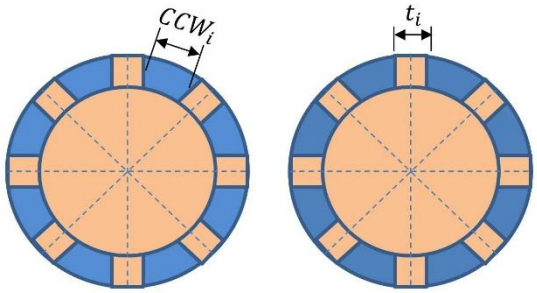

After defining the hydraulic diameter, the Reynolds number at each station $Re_{c,i}$ is defined by

$$Re_{c,i} = \frac{\rho_{c,i} u_{m,i} D_{h,i}}{\mu_{c,i}} = \frac{4\dot{m}_c}{N_i \mu_{c,i} P_i}, \tag{22}$$

where $\rho_{c,i}$ is the specific mass and $u_{m,i}$ is the mean velocity of the cooling propellant at station i. The variable $\dot{m}_c/N_i$ is the mass flow passing through one cooling channel only.

The heat transfer rate at any interface is given by the proper selection of the thermal circuit in Eq. (16). That is

$$q_i = \frac{\left(T_{aw,i} - T_{c,i}\right)}{\left(R_{g,i} + R_{w,i} + R_{c,i}\right)} = \frac{\left(T_{aw,i} - T_{wg,i}\right)}{R_{g,i}} = \frac{\left(T_{aw,i} - T_{wc,i}\right)}{\left(R_{g,i} + R_{w,i}\right)}, \tag{23}$$

where $T_{wc,i}$ is the temperature at the fins bases. Thus, the temperatures $T_{wg,i}$ and $T_{wc,i}$ can then be calculated.

The increase in coolant temperature, as it flows from the nozzle exhaust (*i.e.* $i = n - 1$) to the combustion chamber at the injector plate position (*i.e.* $i = 1$), can be calculated by the energy balance

$$T_{c,i+1/2} = \frac{q_i}{\dot{m}_c c_{p,i}} + T_{c,i-1/2}, \tag{24}$$

where $T_{c,i+1/2}$ and $T_{c,i-1/2}$ are the coolant temperatures exiting and entering the station i, respectively. At $i = n$, the entering temperature is $T_{c,i-1/2} = T_c$, where T_c is the temperature of the coolant fluid entering the cooling channels.

If a sufficient refined grid is used in the longitudinal direction, the mean coolant temperature in each station can be calculated by the arithmetic mean between its entering and exiting values:

$$T_{c,i} = \frac{\left(T_{c,i+1/2} + T_{c,i-1/2}\right)}{2}. \tag{25}$$

Equation (24) clearly forms a recursive relation that can be sequentially used until the coolant reaches the injector plate. As the cooling fluid exits the channels with higher temperature, a more realistic estimative for the combustion gases properties can be obtained with the CEA program. This is not done in the results presented in this work. The Centauri program needs the description of the combustion gases properties in equation form to be directly written on the program lines.

When solving Eq. (16), the heat transfer rate at station i is estimated based on the initial cooling propellant temperature and wall temperatures, $T_{wg,i}$ and $T_{wc,i}$, where $T_{wc,i}$ is the fins bases temperature, as shown in FIGURE 2.

The initial guess for these two temperatures should be consistent. For example, $T_{wg,i}$ in all stations should be equal or just below the gases temperature at its lowest value in the thrust chamber, that is, at T_n. Also $T_{wc,i}$ is expected to be higher than the cooling fluid. It was found that using $T_{wc,i}$ as approximately $100\ K$ above the coolant temperature exiting the cooling channels (i.e. $T_{c,1}$) is sufficient to the iterative process (which is described below) to converge.

The iterative process to calculate the heat transfer and all temperatures in each station proceeds as follows:

1) Calculate properties of the cooling fluid: c_p, $k_{c,i}$, $\mu_{c,i}$ and $Pr_{c,i}$ in all stations based on the estimated $T_{c,i}$;
2) Calculate the hot gases convective heat-transfer coefficient $h_{g,i}$ with Eq. (18-19);
3) Calculate the Reynolds number with Eq. (22) and the hydraulic diameter with Eq. (21);
4) Calculate the coolant convective heat-transfer coefficient $h_{c,i}$ with the Sieder and Tate correlation, Eq. (20);
5) Calculate the fin set efficiency, with Eq. (13-15);
6) Calculate the hot gases thermal resistance, Eq. (10);
7) Calculate the wall thermal resistance, Eq. (11);
8) Calculate the fin set thermal resistance, Eq. (12);
9) Calculate the heat transfer rate with Eq. (16-17) based on the estimative of $T_{c,i}$;
10) Based on the heat transfer rate, estimate the wall temperatures $T_{wg,i}$ and $T_{wc,i}$ choosing the proper terms in Eq. (23);
11) Calculate the coolant temperature exiting each station with the recurrence relation, Eq. (24), from $n \geq i \geq 1$. At $i = n$, the coolant temperature entering the regenerative system equals the coolant feeding system temperature and is an input data of the program (note that the coolant flow is a counterflow);
12) Calculate the new estimative of $T_{c,i}$ with Eq. (25)

13) Return to step 1 until the L^1 non-dimensional norm of the residual of coolant temperature reaches a specified tolerance, typically 10^{-10}.

RESULTS

The fluid flow and thermal resistance models are programmed using the FORTRAN 95 language. As stated before, the resulting program was named Centauri.

The combustion gases pressure and temperature profiles were first validated by means of seven test cases, which were reported in table form in Back, Massier and Gier (1965) for the problem of heated air ($\gamma = 1.345$) flowing through nozzles. The results agreed well with experimental data at the inlet and outlet regions of the nozzle, where the flow is essentially one-dimensional. Near the throat region, where the radial component of velocity is significant, the numerical values are found to be from 4.22 to 5.37% higher than experimental ones. A typical pressure profile, represented by test 262, is shown in FIGURE 4. As the geometry operates as an overexpanding nozzle for the stagnation conditions of this test (P_0 = 518.49 kPa, T_0 = 843.33 K), a recirculation zone develops 0.14 m downstream, increasing the static pressure.

FIGURE 4 – Combustion gases pressure profile.

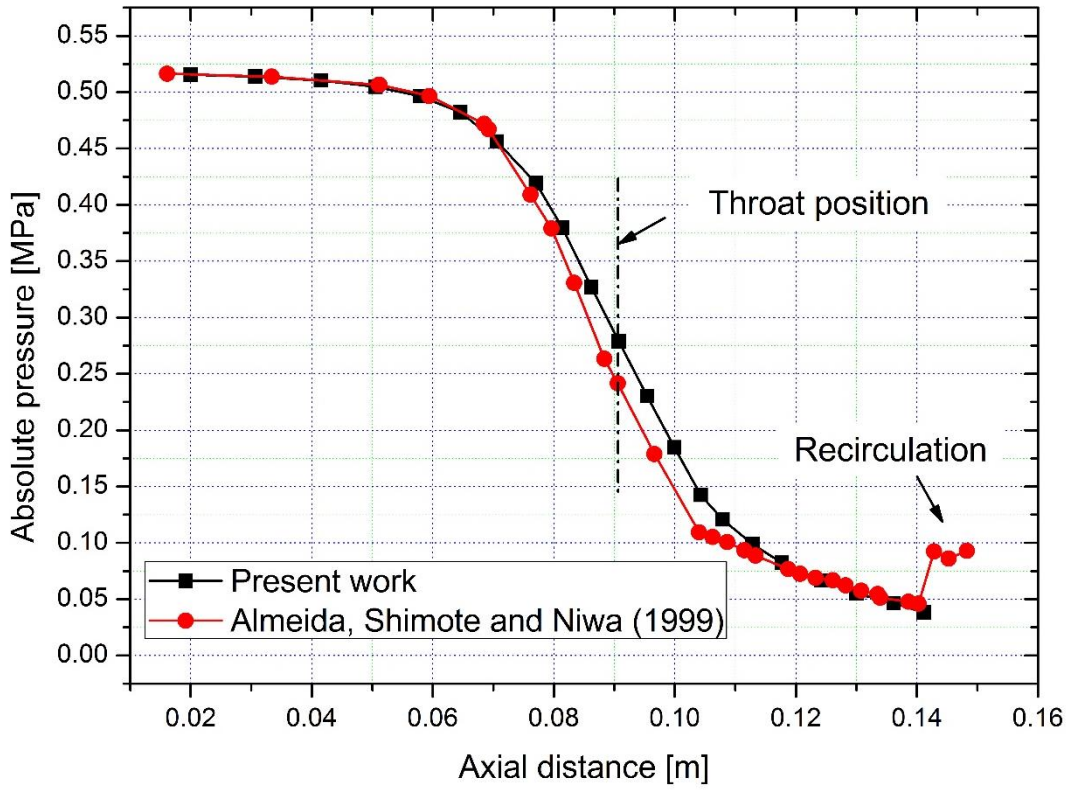

FIGURE 5 shows the results of temperature for test 262. Again, the results agreed well at the converging-diverging nozzle inlet and outlet. Other tests results were very similar to those exposed in FIGURE 4 and FIGURE 5 and are not presented here.

For the simulations of the tests reported in Back, Massier and Gier (1965), the properties of heated air were coded in equation form directly in the source file of the program. Thus, when simulating fluids other than air, the user needs to comment program lines of air and add the suitable equations.

FIGURE 5 – Combustion gases temperature profile.

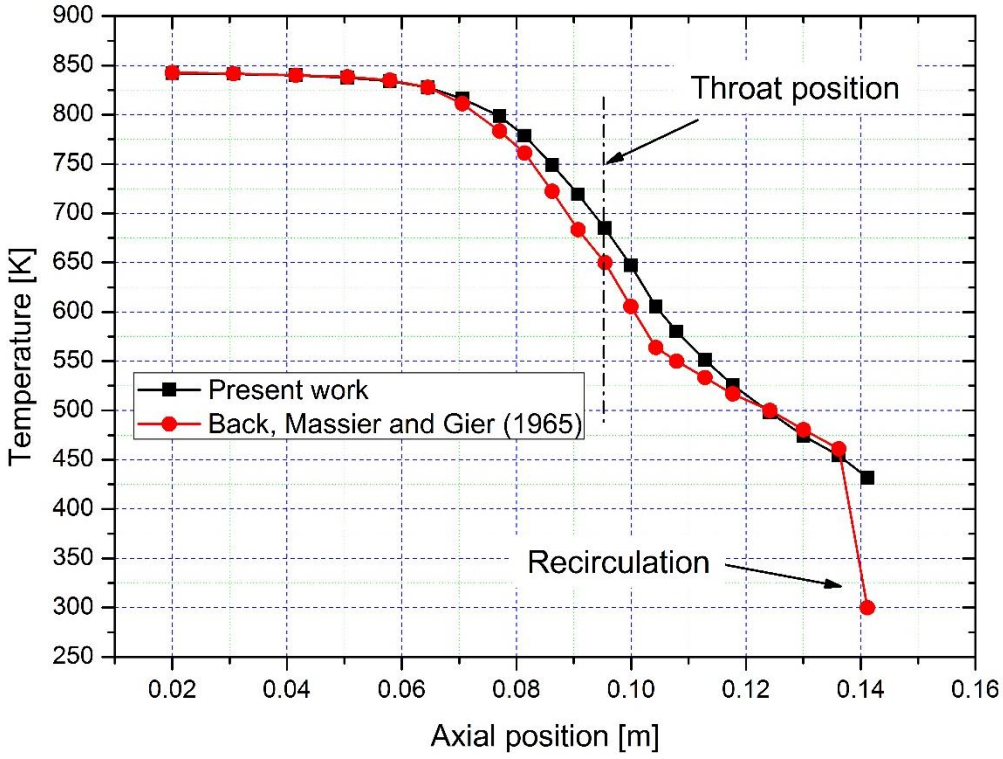

FIGURE 6 shows the convective heat-transfer coefficient of tests 262, 275 and 278 obtained in this work, and their comparison to data extracted from Figure 15 in Back, Massier and Gier (1965). These tests were chosen because the reference paper presents not only the experimental values, but also their results using Eq. (18). This way, they are used to validate results of convective heat-transfer coefficients obtained in this work.

Considering the results of Eq. (18), the largest difference between the results of Back, Massier and Gier (1965) and the ones obtained in this work is 2.83%, and it is observed in test 262. It is important to note that reference results of Eq. (18) were extracted from the original paper in graphical form, thus some error may be expected.

The next step is to validate the iterative procedure that calculates the most important variables of the problem: the heat flux through the wall and the temperatures of the internal wall and coolant. Only the coolant temperature is grid dependent, because the exiting value in each station depends on its value at previous station.

A sufficient refined grid is needed in longitudinal direction to accurately calculate the exiting coolant temperature of each station. The discretization error tends to grow following the coolant flow, so the cooling fluid temperature exiting the thrust chamber is more influenced by such error. Thus, its L^1 non-dimensional norm is monitored until it reaches the convergence criterion that stops the iterative process. It was found that grids with at least 128 stations are sufficiently fine.

FIGURE 6 – Comparison of the convective heat-transfer coefficient obtained from Eq. (18) in this work and the reference paper.

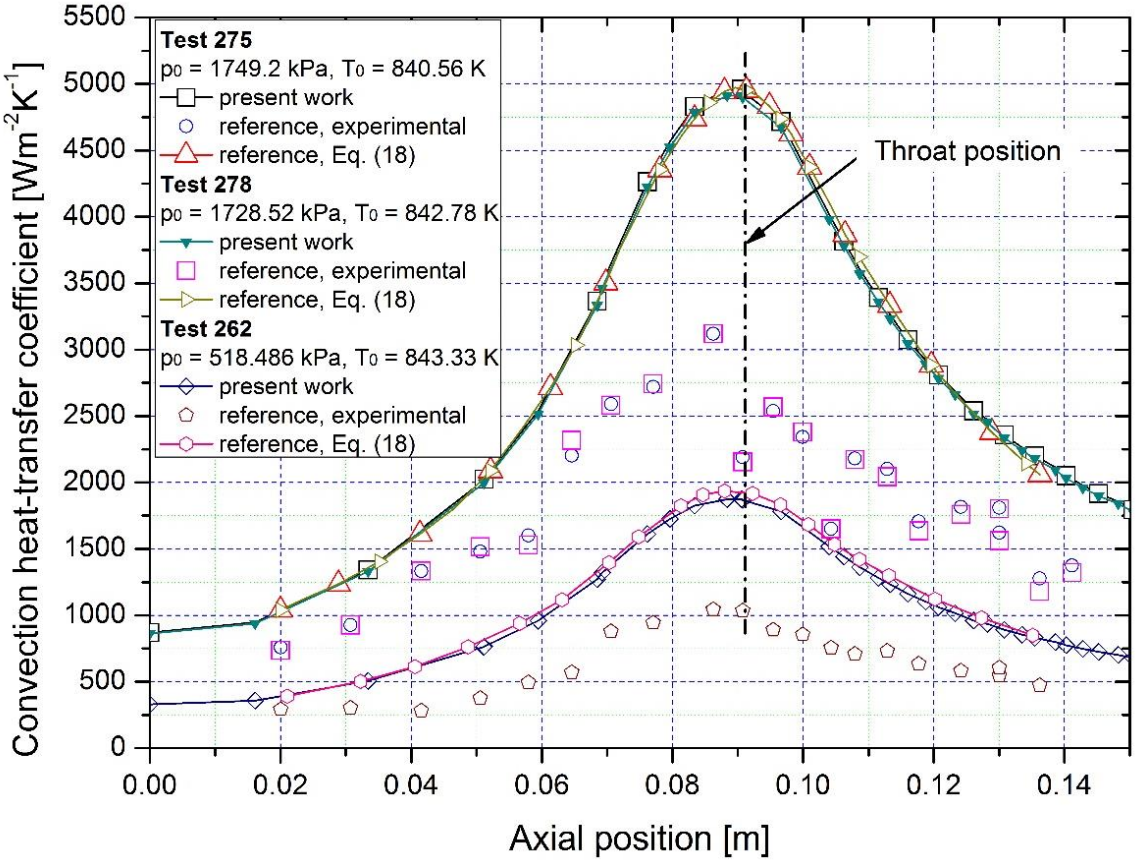

Finding a benchmark engine, where all variables needed for the code validation process is difficult because not only the dimensions and stagnation properties are required, but also the cooling channel geometry, number of channels and cooling fluid properties.

An old version of the L75 rocket engine, described in Almeida, Shimote and Niwa (1999), was chosen to validate the heat flux. The thrust chamber main dimensions and stagnation properties are given in Table 1. As the complete thrust chamber geometry is not available, it was approximated based in Almeida (2003). The coolant is the rocket propellant 1 (RP1), a type of kerosene which properties were taken from the appendix A from Boysan (2008). In this engine, the coolant flows through channels that traverse all the thrust chamber length.

The number of channels in each region is not informed in Almeida, Shimote and Niwa (1999). Instead, the authors mentioned that it produces channels with 2 to 5 mm width. It is found that the pattern described in Table 2 produces channel widths in the range of 2.005 to 4.962 mm. Therefore, this pattern agrees with the last row in Table 1.

Table 1 – L75 input data for simulation

Variable	Value and unit
Oxidizer	Liquid Oxygen
Fuel (coolant)	Kerosene RP1
Coolant flow rate	6.4 kg/s
Coolant entry temperature	303 K
Combustion chamber pressure	6 MPa
Combustion chamber temperature	3605.58 K [1]
Nozzle outlet pressure	7500 Pa
Oxidant / fuel ratio	2.42
Combustion chamber diameter	211 mm
Throat diameter	90 mm
Outlet diameter	719 mm
Combustion chamber length	285 mm
Throat longitudinal position [2]	349 mm
Total thrust chamber length	1491 mm
Internal wall termal conductivity	290 $Wm^{-1}K^{-1}$
Internal wall thickness	1.5 mm
Fin height and width	1.5 mm and 1 mm
Cooling channel width	2 to 5

[1] Obtained with the CEA program.

[2] Assumed value based on Figure 2 from Almeida, Shimote and Niwa (1999) and Almeida (2003).

Table 2 – Number of cooling channels used in the simulation as a function of the longitudinal position

Longitudinal distance from the injector plate [mm]	Number of cooling channels
$z < 293$	170
$293 \leq z < 425$	148
$425 \leq z < 523$	300
$523 \leq z < 1491$	458

The heat flux obtained is shown in FIGURE 7, including the results extracted from Almeida, Shimote and Niwa (1999) in graphical form. As expected, the heat flux is large near the throat, where the mass flow per unit of transversal area reaches its highest value. The combustion chamber has a relatively high heat flux due to the high pressure and temperature upstream the throat. The divergent section has the smallest values due to the relatively low mass flow per unit area combined with relatively low temperature.

It is important to note that only the convective heat transfer is considered inside the thrust chamber in both data sets. If the effect of combustion gases thermal radiation is added to the convective flux, the combined heat flux should be slightly higher in the combustion chamber, but hardly noted in the divergent section.

The different mathematical models used to estimate the convective heat-transfer coefficient could explain the differences observed between both data sets in FIGURE 7. In Almeida, Shimote and Niwa (1999), another mathematical model is used instead of Eq. (18), but not sufficient data is provided in order to use that same model in here. It is well known that Eq. (18) over estimates the convective heat-transfer coefficient as reported in Back, Massier and Gier (1965) and easily noted in FIGURE 6.

FIGURE 7 – Comparison of the heat flux obtained in this work with the reference.

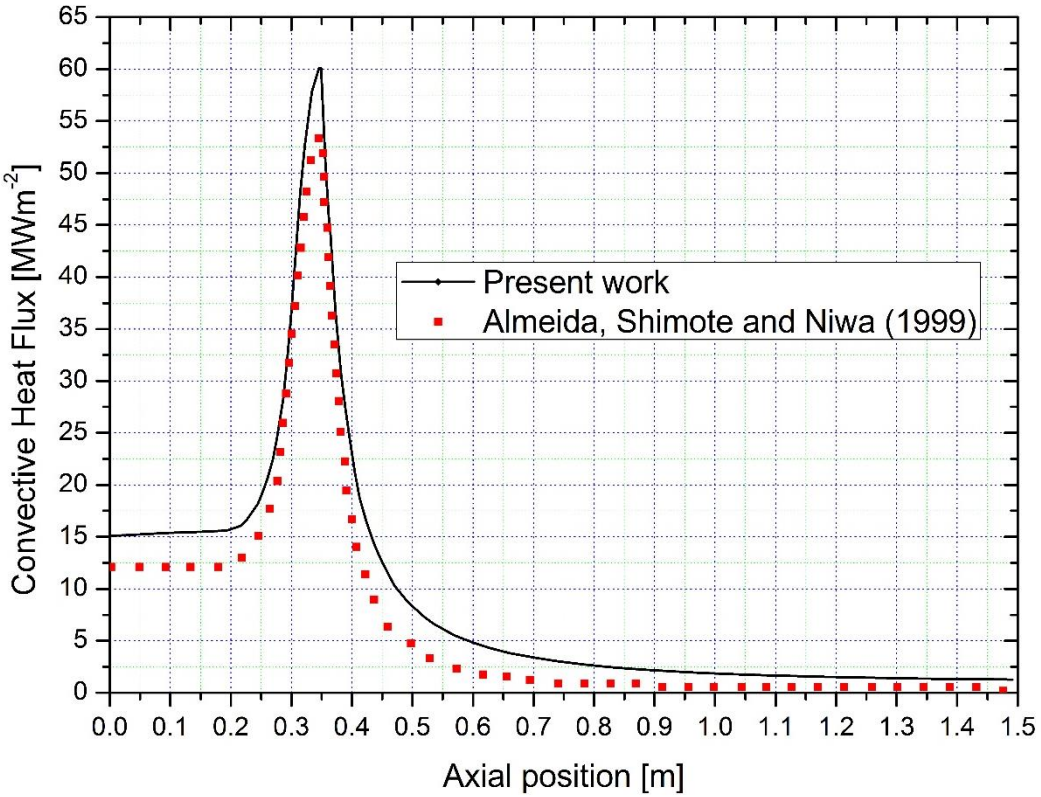

The relative errors between the results in FIGURE 7 are presented in Table 3. It can be noted that significant differences occur in all positions, especially where the flux is small. It is possible that the differences are from both convective heat-transfer coefficient model and the graphical data extraction process.

Table 3 – Heat flux in some positions

Longitudinal distance from the injector plate [mm]	Heat flux (this work) [MW/m^2]	Relative error between present and reference data [%]
0.000	14.57	+20.36
349.0	58.58	+12.81
500.0	8.086	+70.69
1.491	1.161	+561.9

The temperatures profile is shown in FIGURE 8. As expected, the highest temperature occurs in the interface between the internal wall and the combustion gases. The lowest temperature is the coolant bulk temperature. Both these temperatures exceed the practical limits. The internal wall temperature T_{wg} is above the melting point of copper alloys, which are commonly used as internal wall material. In addition, the coolant temperature exceeds its boiling point (SUTTON; BIBLARZ, 2001), and the Eq.(20) does not apply to the boiling regime.

FIGURE 8 – Temperatures profile considering just regenerative cooling and RP1 as cooling fluid. (A brake in the vertical scale can be noted.)

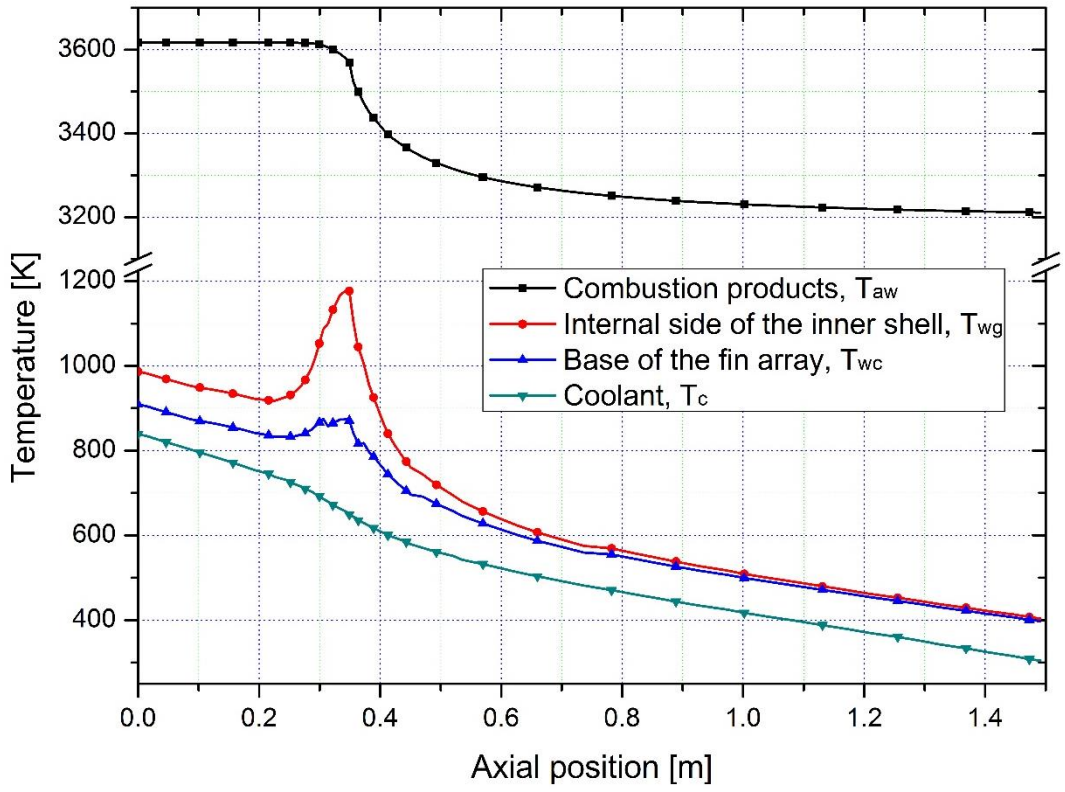

It is obvious that the L75 rocket engine needs cooling strategies other than regenerative cooling. Almeida, Shimote and Niwa (1999) explains that regenerative cooling and film cooling are both used in the studied version

of the L75 engine. As the Centauri does not simulate film cooling, the temperatures shown in FIGURE 8 could not be compared with those presented in that work, therefore they could not be validated.

CONCLUSION

In this work, a numerical code called Centauri was developed to simulate the convective heat transfer inside thrust chambers of rocket engines. The main simplifications hypothesis are the quasi one-dimensional flow of a mixture of gases and the assumption of frozen flow after the throat. The flow is considered a thermal reservoir, so there is no need to update the combustion gases properties inside the iterative loop that calculates the heat transfer rate, wall temperatures and the coolant temperature.

Other simplifications are the constant thermal conductivity of the wall material, no axial conduction between stations and the consideration of outer wall as adiabatic.

The results of fluid flow are consistent with experiments conducted with air heated flowing through nozzles. Some deviation from one-dimensional theory was observed only near the throat, as expected.

The difference between the present results and those from Back, Massier and Gier (1965) for the estimated convective heat-transfer coefficient, Eq. (18), agreed with a difference of 2.83%. The experimental values reported in the reference work are clearly lower than theoretical ones, but the use of Eq. (18) is justified since it estimates heat flux values higher than those occurring in real engines. This procedure can be seen as a safety measure.

The thermal resistance model produces similar values of the heat transfer rate for a kerosene-cooled version of the L75 engine. Despite the heat transfer rate shows similar graphical behavior, the Centauri produces heat flux values 12,81% larger at throat region, 20% larger in the combustion chamber and many times larger in the divergent portion of the nozzle.

The differences between the present work and Almeida, Shimote and Niwa (1999) results are attributed to the use of different models to estimate the convective heat-transfer coefficient and to the process of data extraction, which was made in graphical form. The correspondent temperature profile shows that the internal wall thrust chamber temperature is higher than the melting point of copper alloys, which are commonly employed in rocket engines. In addition, a temperature above the boiling point of the coolant was found. In practical terms, this means that this engine needs cooling techniques combined with regenerative cooling.

ACKNOWLEDGMENTS

Authors thank to the Positivo University. The second author receives a scholarship supported by PROUNI from the Brazilian Federal Government.

REFERENCES

ALMEIDA, D. S. Projeto Motor Foguete a Propelente Líquido L75. In: 7° Seminário de Projetos de Pesquisa e Desenvolvimento em Veículos Espaciais e Tecnologias Associadas. 11-13 set 2013. São José dos Campos, Brazil, 2003.

ALMEIDA, D. S.; SHIMOTE, W.K.; NIWA, M. Selection of materials for combustion chamber of liquid propellant rocket engine. In: **15th Brazilian Congress of Mechanical Engineering**; Águas de Lindoia, Brazil, 1999.

BACK, L. H.; MASSIER, P. F.; GIER, H. L. Convective heat transfer in a convergent-divergent nozzle – Technical report 32-415. Pasadena: **Jet Propulsion laboratory**, 1965.

BORGNAKKE, C.; SONNTAG, R. E. **Fundamentals of thermodynamics**. 7th ed. Hoboken, NJ: John Wiley & Sons, 2009.

BOYSAN, M. E. **Analysis of regenerative cooling in liquid propellant rocket engines** (M. Sc. thesis). Ankara: Middle East Technical University. In English, 2008.

BERGMAN, T. L. et al. **Fundamentals of Heat and Mass Transfer**. 7th ed. Hoboken, NJ: John Wiley & Sons, 2011.

CEARUN: **CEA online**. 02/04/2016. Cleveland (OH): NASA Glenn Research Center; [Accessed 2017 Mar 21]. https://cearun.grc.nasa.gov.

CHAPRA, S. C.; CANALE, R. P. **Numerical methods for engineers**. 7th ed. New York: McGraw-Hill Education, 2015.

GORDON, S.; MCBRIDE, B. J. Computer program for calculation of complex chemical equilibrium compositions and applications – Part I Analysis. Cleveland: **NASA Lewis Research Center**, 1994.

HOWELL, J. R.; STRITE, M. K.; RENKEL, H. E. Analysis of heat-transfer effects in rocket nozzles operating with very-high temperature hydrogen. Cleveland: **NASA Lewis Research Center**, 1965.

MCBRIDE, B. J.; GORDON, S. Computer program for calculation of complex chemical equilibrium compositions and applications – Part II users manual and program description. Cleveland: **NASA Lewis Research Center**, 1996.

NARAGHI, M. H.; FOULON, M. A simple approach for the thermal analysis of regenerative cooling of rocket engines. Paper presented at **2008 ASME international Mechanical Engineering Congress and Exposition**, Boston, United States of America.

NARAGHI, M. H.; ARMSTRONG, E. S. Three dimensional thermal analysis of rocket thrust chambers. Paper presented at: **Thermophysics, Plasmadynamics and lasers conference**; San Antonio, United States of America, 1988.

SUTTON, G. P.; BIBLARZ, O. **Rocket propulsion elements**. 8th ed. Hoboken, NJ: John Wiley & Sons, 2010.